A PROBABILISTIC APPROACH TO PREDICT CRACKING IN LIGHTLY REINFORCED MICROCONCRETE PANELS

Ana Rita Cordeiro da Silva, Sergio Proença, René Billardon, François Hild

Submitted to the Journal of Engineering Mechanics, August 2002
Revised February 2004 (EM-23284)

A PROBABILISTIC APPROACH TO PREDICT CRACKING IN LIGHTLY REINFORCED MICROCONCRETE PANELS

by

Ana Rita C. da Silva,[1] Sergio P.B. Proença,[2] René Billardon[3] and François Hild[4,*]

[1]Post-doctoral fellow, Department of Structural Engineering, São Carlos School of Engineering
University of São Paulo, Avenida do Trabalhador São Carlense 400, 13560-590 São Carlos, SP, Brazil

[2]Professor, Department of Structural Engineering, São Carlos School of Engineering
University of São Paulo, Avenida do Trabalhador São Carlense 400, 13560-590 São Carlos, SP, Brazil

[3]Professor, LMT-Cachan, ENS de Cachan / CNRS-UMR 8535 / Université Paris 6
61 avenue du Président Wilson, F-94235 Cachan Cedex, France

[4]Research professor, LMT-Cachan, ENS de Cachan / CNRS-UMR 8535 / Université Paris 6
61 avenue du Président Wilson, F-94235 Cachan Cedex, France

[*]To whom correspondence should be addressed
Fax: +33 1 47 40 22 40, Email: hild@lmt.ens-cachan.fr

A PROBABILISTIC APPROACH TO PREDICT CRACKING IN LIGHTLY REINFORCED MICROCONCRETE PANELS

by

Ana Rita Cordeiro da Silva, Sergio P.B. Proença, René Billardon and François Hild

Abstract

The ultimate strength of structures made of brittle materials –such as microconcrete– strongly depends on microstructural defects, the structure size and the loading pattern. Probabilistic approaches allow one to take account of such dependencies. By using a Weibull model, cracking of ferrocement panels is analyzed. Provided the behavior of the reinforcement remains elastic, it is shown that the Weibull parameters identified on unreinforced microconcrete samples tested in flexure may be used to predict multiple cracking in ferrocement panels tested in tension. A key aspect of the analysis is related to the understanding and modeling of the stress heterogeneity effect on the local failure probability of unreinforced as well as reinforced microconcrete by the use of a so-called Weibull stress.

CE Database Subject Headings:

Concrete, reinforced, Cracking, Probabilistic methods, Scale effect.

INTRODUCTION

Ferciment (i.e., "ferrocement") was invented 150 years ago by Lambot who, in 1845 constructed pots and seats, and built a boat with this material in 1848. A first patent on the mixed use of iron and cement was made in 1851 and *ferciment* is patented since 1855 (Lambot 1855; Marrey 1995). Its utilization for structural purposes only started in 1943 thanks to Nervi's contributions (1951). Ferrocement is the oldest form of reinforced concrete and is composed of a cement-based mortar or concrete matrix reinforced with a mesh of closely spaced iron rods or wires (Naaman 2000). Nowadays many civil engineering applications use some kind of (fiber-)reinforced concrete or cement (Balaguru and Shah 1992). The interest in these materials is due to the gain in toughness and ductility in the presence of cracks that are bridged by the reinforcements. Furthermore, lightly reinforced microconcrete has been developed as a low-cost material to be used in thin-walled structural components [e.g., pre-formed skeleton (El Debs 2000)]. The strength and deformability of these structures are improved when compared to conventional "ferrocement" (Hanai and El Debs 1994). The prediction of cracking in such structural components is essential for design purposes and this constitutes the main goal of the present paper.

The understanding of the basic mechanisms and the modeling of the mechanical properties, such as the tensile response, of ferrocement and other brittle matrix composites reinforced with continuous fibers are issues that have been addressed by many authors (Naaman 2000). Deterministic tensile strength values have been proposed on the basis of standard direct or indirect experiments and then corrected by empirical factors to account for scale and stress heterogeneity effects. However, the resulting values and its representativity are still a subject of discussion. Modeling the tensile response of ferrocement by a probabilistic approach is an alternative that has not been considered. It is proposed to

evaluate the predictive capability of a Weibull model to describe cracking of lightly reinforced microconcrete panels.

The identification of constitutive equations of mortar and unreinforced concrete in tension is difficult to carry out because of strain localization leading to the formation of a single macrocrack. A so-called *single cracking* regime prevails and alternative techniques have been proposed to avoid it in experiments. One of them consists in adding primary reinforcements acting like fibers in a composite material. Inspired by the experimental analysis of L'Hermite (1960), a special tension test designed to prevent single cracking was devised by Bažant and Pijaudier-Cabot (1989) and modified by Mazars and colleagues (1989; 1990). In that case, *multiple macrocracking* can be observed. The analysis of this type of experiment requires to account for the behavior of the interface between the primary reinforcement and the tested brittle material (Boudon–Cussac et al. 1999).

In the present work, the spirit of the above-mentioned experimental technique is followed. Contrary to experiments on unreinforced concrete or mortar, it will be assumed that the reinforcements, even though in low volume fraction, will be sufficient to prevent single cracking. It is proposed to predict cracking in panels made of lightly reinforced microconcrete from the analysis of the failure of unreinforced concrete beams and steel reinforcements. A probabilistic analysis of the failure of a brittle matrix made of concrete with a controlled aggregate distribution is presented. Following the work of Kadlecek and Spetla (1967) and L'Hermite (1973), the experimental investigation aims at analyzing the scale effects in brittle materials, namely volume and stress heterogeneity effects. A Weibull model (1939) is chosen to describe the scatter of failure stresses in three- and four-point flexure. The failure properties of the reinforcements used in the present analysis are evaluated. Experiments and predictions of the cracking regime in lightly reinforced concrete panels are reported. In

particular, a probabilistic approach is developed to analyze the conditions for single and multiple cracking.

PROBABILISTIC APPROACH TO THE FAILURE OF MICROCONCRETE

The failure stress measurements for the microconcrete studied herein are scattered. Consequently a Weibull model is used to account for the scatter of the failure stress as well as volume and stress heterogeneity effects. It can be noted that the Weibull model mainly describes the crack initiation conditions. It has been shown to be relevant for ceramics (Jayatilaka 1979), glasses (Kurkjian 1985), and brittle metals (Beremin 1983). However, for quasi-brittle materials such as (reinforced) concrete, it has been shown that the so-called size effects are not necessarily realistic (Bažant 1984; 2000) because a whole process zone develops prior to failure instead of a single cracking event. In the present study, a microconcrete is considered with weak failure properties that may be analyzed by the simple Weibull model.

Weibull Model

In the present section, a Weibull (1939) analysis is performed to model the fracture properties of unreinforced microconcrete samples. The analysis is based upon the weakest link hypothesis (Freudenthal 1968). For unreinforced brittle materials, it is assumed that a single cracking regime occurs (i.e., the initiation and propagation of a single macroscopic crack leads to the failure of the structure). Consequently, the cumulative failure probability P_F of a domain Ω can be expressed as

$$P_F = 1 - \exp\left[-\frac{1}{V_0} \int_{\Omega} \left(\frac{\langle \sigma_e(\mathbf{x}) \rangle}{S_0} \right)^m d\mathbf{x} \right]. \quad (1)$$

Equation (1) corresponds to a two-parameter Weibull model in which the two independent parameters are the Weibull modulus *m* (describing the scatter) and the scale parameter $V_0 S_0^m$ (i.e., V_0 and S_0 cannot be identified separately; usually an *a priori* value is chosen for V_0 and S_0 is tuned). The failure stress is defined as the maximum value of the equivalent stress over the domain Ω

$$\sigma_F = \max_{\Omega} \sigma_e(\mathbf{x}) . \tag{2}$$

Equation (1) can be used to define the effective volume (Davies 1973) and the stress heterogeneity factor (Hild et al. 1992)

$$V_{eff} = \int_{\Omega} \left(\frac{\langle \sigma_e(\mathbf{x}) \rangle}{\sigma_F} \right)^m d\mathbf{x} = V H_m , \tag{3}$$

so that

$$P_F = 1 - \exp\left[-\frac{V_{eff}}{V_0} \left(\frac{\langle \sigma_F \rangle}{S_0} \right)^m \right] . \tag{4}$$

The so-called Weibull stress (Beremin 1983) is defined as

$$\sigma_w = \sigma_F \left(\frac{V_{eff}}{V_0} \right)^{1/m} . \tag{5}$$

It can be noted that, according to the Weibull model, the experimental data should be aligned according to the following *linear* interpolation

$$\ln\left[\ln\left(\frac{1}{1-P_F} \right) \right] = m\left(\ln \sigma_w - \ln S_0 \right), \tag{6}$$

where the slope is the Weibull modulus *m* and the x-intercept is $\ln S_0$. Furthermore, the average failure stress can be derived as

$$\overline{\sigma}_F = S_0 \left(\frac{V_0}{V_{eff}} \right)^{1/m} \Gamma\left(1+\frac{1}{m}\right). \quad (7)$$

It can be noted that the ratio V_{eff}/V_0 only depends on the Weibull modulus m. In the following, the cumulative failure probability relative to a batch of experiments is defined by (Jayatilaka 1979)

$$P_F = \frac{i}{N+1}, \quad (8)$$

corresponding to the arranged failure stresses σ_{Fi} in ascending order

$$\sigma_{\mathrm{F1}} < \sigma_{\mathrm{F2}} < \ldots < \sigma_{\mathrm{Fi}} < \ldots < \sigma_{\mathrm{FN}}. \quad (9)$$

Once the failure probabilities are known, the Weibull parameters can be tuned by using a least squares fit of Eqn. (6).

Experimental Results

Microconcrete samples are made of materials with special proportions (1 volume of cement, 2.67 volumes of sand, 1.33 volumes of aggregates and 0.80 volume of water) so that the strength is sufficiently low for panels to be analyzed herein (i.e., with a low volume fraction of reinforcements). Furthermore, the sand distribution was controlled by using different sieve sizes. Table 1 shows the size distribution for the sand of the region of São Carlos (SP, Brazil) used in the experiments. An average size of 0.6 mm is obtained. Similarly, the size distribution of aggregates was measured (Table 2) and an average size of 2.8 mm is found. The average compressive strength of 3 standard samples (diameter: 10 mm, height, 28 mm) tested 41, 69, 97 and 132 days after casting is equal to −17.5 MPa, whereas the average value of Young's modulus is equal to 19 GPa (Silva 2002).

Four series of experiments have been carried out on microconcrete samples. Two different sample sizes, namely 25 x 25 x 170 mm^3 and 25 x 25 x 320 mm^3, and two different types of loadings, namely three-point flexure (outer span: 150 mm and 300 mm, respectively) and four-point flexure (outer span: 150 mm and 300 mm, respectively, inner span: 50 mm and 100 mm, respectively) have been considered. For each series, four different ages of the same batch of material have been tested (i.e., 41, 69, 97 and 132 days after casting). Each test consists of 10 samples (total number: 10 x 4 x 4 = 160). The tests were carried out on a servo-hydraulic testing machine with a controlled stroke rate of 0.25 μm/s. The maximum load is recorded and a classical beam theory solution (Gere and Timoshenko 1997) is used to evaluate the maximum tensile stress [or failure stress, see Eqn. (2)].

Effect of Age

Figure 1 shows the results of one set of experimental data obtained for four different ages of a single batch of microconcrete. No direct correlations between strength and age can be inferred from the present results. This trend was observed for virtually all four series of experiments (Silva 2002). Consequently, for each series of 40 experiments, no age distinction will be made. The only difference is given by the volume and type of loading between the four sets of experiments. This effect is discussed by using the Weibull model.

Model Identification

Each set of experiments is analyzed separately to determine the corresponding Weibull parameters. To perform the identification, the following stress heterogeneity factors were used for a beam theory solution in four-point flexure (outer span / inner span = 3, see Appendix)

$$H_m = \frac{1}{6(m+1)} + \frac{1}{3(m+1)^2}, \tag{10}$$

and three-point flexure

$$H_m = \frac{1}{2(m+1)^2}\,. \tag{11}$$

Figure 2 shows the predictions of the model for each series of tests compared with experimental data. The failure probabilities are evaluated by using Eqn. (8) for each series when the failure stresses are ranked in ascending order [see Eqn. (9)]. A reasonable agreement is obtained (i.e., a correlation coefficient at least equal to 0.96). Table 3 summarizes the values of the Weibull parameters for a reference volume arbitrarily chosen (i.e., $V_0 = 20\,\mathrm{cm}^3$). Even though the values are not identical, the order of magnitude is the same. However, the number of experiments remains small for each series so that the determination of the Weibull parameters is not very accurate (Absi et al. 1999). In the following, it is proposed to use the Weibull stress to analyze all the experimental data as a single set of experiments on the same material since different load patterns can be compared in a unified way by means of the effective volume.

Only one set of Weibull parameters is used to describe the failure properties of the microconcrete matrix. To start the identification, an initial Weibull modulus is needed (e.g., $m = 5.3$) so that the Weibull stresses [Eqn. (5)] for each experimental point can be determined by computing the effective volume. The stresses are then arranged in ascending order and a new identification of the two Weibull parameters is possible. For any of the four Weibull moduli taken as initial value, two iterations are needed to converge to the following values: namely, $m = 7.3$ and $S_0 = 4.0\,\mathrm{MPa}$. It can be noted that these values are very close to the average obtained for the four sets of experiments (i.e., $m = 7.3$ and $S_0 = 4.1\,\mathrm{MPa}$). Figure 3 shows the results obtained with this procedure in which all the data are considered simultaneously. A very good agreement is obtained (i.e., a correlation coefficient greater than 0.99). This result shows that the Weibull stress is a useful tool to analyze different types of experiments on different loaded volumes as one single set of experimental data points.

Lastly, it can be noted that the model describes reasonably well the volume effect (i.e., the larger the volume, the lower the average failure stress). This is especially noticeable for 4-point flexure specimens that experience the lower stress heterogeneity (see Table 3). The stress heterogeneity effect is also reasonably well modeled (i.e., the higher the stress heterogeneity, the lower the stress heterogeneity factor, and the higher the average failure stress). Table 3 shows that the prediction by the Weibull model of the average failure stress is such that the maximum difference with the experimental value is less than 10% of the experimental average strength.

This first analysis allows us to conclude that the Weibull model leads to reasonable estimates of the failure properties of the microconcrete studied herein for effective volumes varying between 0.68 cm^3 (i.e., small samples loaded in 3-point flexure) and 4.67 cm^3 (i.e., large samples loaded in 4-point flexure).

FAILURE PROPERTIES OF THE REINFORCEMENTS

The reinforcements are wires 3.8 mm in diameter made of low carbon steel (wt%: C = 0.08-0.13, S ≤ 0.03, Mn = 0.3-0.6, P ≤ 0.03, Si = 0.1-0.2, Al ≤ 0.008, Fe = balance). Two different lengths are tested. For each series, 10 different experiments are carried out (total number: 20). Tensile tests are performed with a servo-hydraulic testing machine with a controlled stroke rate of 5 μm/s. The strains are measured with a clip gauge (gauge length: 25 mm). Contrary to the previous case, it is expected that the overall strength of the reinforcements does not follow a Weibull model. This is confirmed by analyzing the data reported in Table 4 since no significant volume effect is observed. This result was confirmed by another series of experiments on wires 2.5 mm in diameter (Silva 2002). The average tensile strength is of the order of 870 MPa with an average Young's modulus of 210 GPa. For a frame made of a perpendicular array of 8 welded wires (spacing between wires:

S = 100 mm, wire diameter: d = 3.8 mm, see Fig. 4), the ultimate strength is given equal to 895 MPa in the longitudinal direction, and 870 MPa in the transverse direction. It can be noted that these values are close to those found for pristine wires.

This second study shows that, as expected, a purely deterministic approach can be used to analyze the ultimate tensile strength of the steel grid to be utilized in the lightly reinforced microconcrete panels.

CRACKING IN LIGHTLY REINFORCED MICROCONCRETE PANELS

In the present section, one set of 33 panels is analyzed (panel size: 400 x 400 x 25 mm^3). The matrix is identical to that studied previously. The reinforcement consists of a grid of welded steel wires analyzed above. Figure 4 shows a schematic view of the sample geometry. A very small volume fraction of reinforcement is used, namely f = 0.005. The first part of this section discusses the conditions to obtain multiple cracking for reinforced microconcrete when the matrix cracking stress is random. The second part is devoted to the extension of the cracking conditions to the panels when they are loaded by the longitudinal wires. The third part discusses the experimental measurements used to evaluate the induced flexure caused by the experimental procedure. As a consequence, the analysis of the cracking stresses requires using the approach with the Weibull stress.

Single and Multiple Matrix-Cracking of Reinforced Concrete

Following the analysis initially proposed by Aveston et al. (1971; 1973), we consider an elementary cell (Fig. 5) consisting of a continuous reinforcement (Young's modulus E_s and volume fraction f) embedded in a matrix (Young's modulus E_c and volume fraction 1–f). Before cracking, perfectly bonded interface is assumed so that the longitudinal strains are identical in the matrix and the reinforcement. The applied stresses are assumed to be uniaxial

and uniform in each section. When no cracking occurs, the macroscopic Young's modulus is assumed to be equal to

$$E = (1-f)E_c + fE_s\,, \tag{12}$$

so that the stress in the reinforcement is expressed as

$$\sigma_s = \Sigma \frac{E_s}{E}, \tag{13}$$

and that in the matrix as

$$\sigma_c = \Sigma \frac{E_c}{E}\,. \tag{14}$$

Hence, the applied stress Σ is related to σ_s and σ_c by

$$f\sigma_s + (1-f)\sigma_c = \Sigma\,. \tag{15}$$

As was shown previously, the matrix is weaker than the reinforcement. Multiple matrix-cracking will occur when the first matrix crack does not lead to the failure of the reinforcement bridging the crack. This result is applied to the elementary cell of Fig. 5. If the strength $f\sigma_{su}$ is less than the stress level at which matrix-cracking occurs $\Sigma_{cr} = \sigma_{cu} E/E_c$, there will be single matrix-cracking. Conversely, when

$$f > f_{cr} = \left(\frac{\sigma_{su}}{\sigma_{cu}} + 1 - \frac{E_s}{E_c} \right)^{-1}, \tag{16}$$

multiple matrix-cracking is expected. To obtain the previous results, the failure strengths of the matrix and the reinforcements were assumed to be deterministic. In practice, this hypothesis is only a simplification. In the present case, only the matrix strength is considered to be of random nature. A first modification would be to replace in Eqn. (16) the failure stress

of the matrix σ_{cu} by its average $\overline{\sigma}_{cu} = S_0 \left(\frac{V_0}{V_c} \right)^{1/m} \Gamma\left(1 + \frac{1}{m}\right)$ so that the volume effect can be accounted for. Another alternative consists in associating to each failure stress of the matrix σ_{cu} a cracking probability P_{cr} that can be described by a two-parameter Weibull model (see Eqn. (4) with $V_{eff} = V_c$)

$$\sigma_{cu}(P_{cr}) = S_0 \left(\frac{V_0}{V_c} \right)^{1/m} \left[-\ln(1 - P_{cr}) \right]^{1/m}, \tag{17}$$

so that the critical volume fraction is defined in terms of the first matrix-cracking event in the composite

$$f_{cr}(P_{cr}) = \left(\frac{\sigma_{su}}{S_0 \left(\frac{V_0}{V_c} \right)^{1/m} \left[-\ln(1 - P_{cr}) \right]^{1/m}} + 1 - \frac{E_s}{E_c} \right)^{-1}. \tag{18}$$

Figure 6 shows the different cracking regimes for a unidirectional reinforced brittle matrix whose properties are those obtained in the two previous sections (namely, $E_s = 210\,\text{GPa}$, $E_c = 19\,\text{GPa}$, $\sigma_{su} = 810\,\text{MPa}$, $S_0 = 4.0\,\text{MPa}$, $m = 7.3$) and subjected to tension. Above a given curve, a multiple cracking regime is expected, whereas below that line, a single cracking regime occurs. For instance, for a reinforcement volume fraction $f = 0.005$, multiple matrix-cracking is likely to occur (i.e., $f > f_{cr}$) for a probability P_{cr} of 72 % when the volume of the matrix is equal to the reference volume (i.e., $V_c / V_0 = 1$). Furthermore, the higher the volume V_c, the lower the failure stress for the same failure probability [see Eqn. (4)], therefore the more likely multiple matrix-cracking. This result is valid provided the composite is subjected to a uniform tensile stress. If the stress field is heterogeneous, the

above-mentioned conclusion can be utilized by considering the effective volume $V_c H_m$ instead of the volume V_c as will be shown below.

It can be noticed that these developments constitute a *probabilistic* treatment of single and multiple cracking in reinforced brittle matrices whereas all failure strengths were *deterministic* in the original analysis of Aveston et al. (1971; 1973).

Single and Multiple Matrix-Cracking in Lightly Reinforced Microconcrete Panels

In practice, the steel grid used herein (Fig. 4) induces a loss of symmetry of the microconcrete panels when loaded by the longitudinal wires because of the eccentricity δ. Consequently, the previous analysis has to be adapted to account for induced flexure coupled with tension. A simplified analysis with a linear distribution of strain in the loading direction is undertaken. It is therefore assumed that all the longitudinal wires are equally loaded in this first analysis. In the loaded volume, the longitudinal strain field is assumed to be given by

$$\alpha\varepsilon_{\max} \le \varepsilon_{yy}(x) = \left[\frac{1+\alpha}{2} + (1-\alpha)\frac{x}{h}\right]\varepsilon_{\max} \le \varepsilon_{\max} \text{ when } -h/2 \le x \le h/2\,. \tag{19}$$

The flexure parameter α has to be related to the eccentricity δ. The transverse wires (i.e., aligned along the *z* direction) are not modeled. However, it is assumed that thanks to their presence, Eqn. (19) constitutes a good approximation of the longitudinal strain field in an equivalent beam for which the elastic behavior in the transverse (*z*) direction is homogenized for $\delta - d/2 \le x \le \delta + h/2$. The equivalent Young's modulus in this homogenized region is computed as (Fig. 4)

$$E_h = (1-f_h)E_c + f_h E_s\,, \tag{20}$$

where the apparent surface fraction of reinforcements is defined as (Fig. 4)

$$f_h = 2\left(\frac{\pi d^2}{4}\right)\frac{1}{2Sd} = \pi d / 4S\,. \tag{21}$$

The eccentricity δ induces a flexural moment δF (Fig. 4) leading to the following relationship between δ and α

$$\alpha = \frac{\left[\frac{1}{12}\left(h^2 - \frac{d^3}{h}\right) - \frac{\delta}{2}(h-d)\right]E_m + \left(\frac{d^3}{12h} - \frac{d\delta}{2}\right)E_h}{\left[\frac{1}{12}\left(h^2 - \frac{d^3}{h}\right) + \frac{\delta}{2}(h-d)\right]E_m + \left(\frac{d^3}{12h} + \frac{d\delta}{2}\right)E_h}. \tag{22}$$

In Fig. 7, the flexure parameter α is plotted as a function of the eccentricity δ by using the present material parameters. When the eccentricity δ varies between 4 and 0 mm, the flexure parameter α varies between 0 and 1. In particular, when the symmetry axis of the wire frame coincides with the mid-section axis of the panel (i.e., $\delta = d/2 = 1.9$ mm) a value of 0.35 is obtained. For this value, one can evaluate *a priori* the effective volume in a 'tensile' test of the panels. By using Eqns. (3) and (19) and neglecting the reinforcement stress contribution (since f is very small), the following stress heterogeneity factor is found (see Appendix)

$$H_m(\alpha) = \begin{cases} \dfrac{1-\alpha^{m+1}}{(m+1)(1-\alpha)} & \text{when } \alpha \geq 0, \\ \dfrac{1}{(m+1)(1-\alpha)} & \text{otherwise.} \end{cases} \tag{23}$$

Equation (23) shows that the lower α, the lower the stress heterogeneity factor and the higher the average failure stress [see Eqn. (7)]. By assuming that the relevant volume to consider is V_c = 300 x 300 x 25 mm^3, the dimensionless effective volume $V_c H_m / V_0$ is of the order of 20 and a multiple cracking regime is to be expected (Fig. 6) for the present reinforcement volume fraction (i.e., of the order of 0.005).

This second part shows that even though a uniaxial load is applied, which usually corresponds to pure tension, the asymmetry of the panel architecture induces flexure in the

microconcrete matrix. A stress heterogeneity factor has to be evaluated to be able to compute a quantity that is relevant for the cracking analysis, i.e. the effective volume $V_c H_m$.

Experimental Measurements

Equation (23) shows that an accurate estimate of α is needed to analyze the experiments on panels. To evaluate α, six transducers are used, three per analyzed surface (Fig. 8). First, from the two groups of three measurements on each surface, an average signal is determined (i.e., U_L and U_R). From these two signals, an *apparent* coefficient of flexure α_a is determined (when $U_L \le U_R$)

$$\alpha_a = \frac{U_L}{U_R}. \tag{24}$$

Since the measurement is performed at a distance $b = 40$ mm from the surface (Fig. 8), the parameter α_a is different from α. The displacements U_L and U_R not only include the strains in the panel, but also the rotation of the sections described by an angle θ with respect to the axis of symmetry of the panel. The angle θ can be expressed in terms of the thickness of the panel h and the distance b

$$\tan\theta = \frac{U_L - U_R}{2(2b+h)}, \tag{25}$$

so that the actual flexure coefficient α can be deduced

$$\alpha = \frac{\alpha_a(h+b)+b}{\alpha_a b + (h+b)}. \tag{26}$$

Similarly, one can determine a flexure parameter β in the other plane by a linear interpolation of the three measurements per face. This second parameter accounts for the fact that the four longitudinal wires are not uniformly loaded. Equation (19) is therefore generalized to become

$$\varepsilon_{yy}(x,z)=\left[\frac{1+\alpha}{2}+(1-\alpha)\frac{x}{h}\right]\left[\frac{1+\beta}{2}+(1-\beta)\frac{z}{L}\right]\varepsilon_{\max}. \tag{27}$$

Consequently, the stress heterogeneity factor becomes

$$H_m(\alpha,\beta)=H_m(\alpha)H_m(\beta), \tag{28}$$

where $H_m(.)$ is defined in Eqn. (23). Figure 9 shows an example of six displacement measurements and the reconstructed strains used to determine α and β. In this particular example, an apparent coefficient of flexure $\alpha_a \approx -0.24$ is found, whereas $\alpha \approx 0.44$ and $\beta \approx 0.75$. When the value of the flexure parameters α and β are known, one can determine the maximum stress in the matrix when the first matrix crack appears. In Fig. 9, one can see a load drop that can be related to the initiation and propagation of the first matrix crack. Let F_1 be the load level prior to the first load drop. The corresponding average tensile stress is given by $\Sigma_1 = F_1/hL$. The maximum tensile stress in the matrix, σ_1, is related to Σ_1 by

$$\sigma_1 = E_c\varepsilon_{\max} = \frac{4\Sigma_1 E_c}{(1+\alpha)(1+\beta)E}, \tag{29}$$

since the average strain in the matrix is such that $\bar{\varepsilon}_m \approx \varepsilon_{\max}(1+\alpha)(1+\beta)/4$.

Beyond the first cracking event, the displacement measurement now includes the crack opening displacement when the crack is located within the measurement zone. Subsequently, the analysis of the second and third cracking events requires additional hypotheses to be made since only global measurements are performed. One can make one of the following three different sets of assumptions:

- the crack opening displacement is identical on both surfaces of the panel. Equation (26) is still valid to determine the flexure parameter α and the elastic analysis can still be performed in the undamaged volume. Furthermore, as suggested by the observation of many of the tested panels, the first crack is supposed to be located along one of the

transverse wires that are close to the lower or upper surface, and the other successive cracks are supposed to occur along one of the other transverse wires. According to such hypotheses, the undamaged volume can be assumed to be V_c = 200 x 300 x 25 mm^3 for the second cracking event and V_c = 100 x 300 x 25 mm^3 for the third cracking event.

- the first value of the flexure parameter α remains identical during the whole test. Consequently, the analysis performed for the first cracking event can be repeated for the second and third ones by using Eqns. (26) and (27) with the value of α measured for the first load drop.
- when a crack is located within the measurement zone, the flexure parameter α is kept constant throughout the subsequent analysis and equal to the value recorded prior to the cracking event. Conversely, when no crack is located in the measurement zone, the flexure parameter can be evaluated again prior to a new cracking event. It could be checked that in that case the value of α did not evolve significantly, thereby validating the hypothesis made when cracking occurred within the measurement zone. The same type of analysis is performed for the parameter β. To evaluate the effective volume, it is assumed that the elastic analysis can be performed in the undamaged volume that is defined as V_c = 300 x 300 x 25 mm^3 for the first cracking event, V_c = 200 x 300 x 25 mm^3 for the second cracking event and V_c = 100 x 300 x 25 mm^3 for the third cracking event.

This last choice will be made in the following study. The present analysis shows that with a limited number of measurements, the cracking scenario cannot be inferred in a direct way.

Prediction of the Cracking Stresses

Each of the 33 panels that have been tested exhibits a different value of α for the cracking events. In Fig. 7, the values of α corresponding to the first matrix crack are plotted

and the eccentricities deduced from Eqn. (22). The values α were obtained by using the strain measures [Eqn. (24)] and the correction given by Eqn. (26). As anticipated, these values are scattered. Yet the range of values allows us to conclude that the samples did not experience compressive stresses since α remains positive. The mean value of α is equal to 0.33 and that of the eccentricity δ is of the order of 2 mm (corresponding standard deviation: 0.7 mm). This value must be compared to the value $\delta = 1.9$ mm (i.e., $\delta = h/2$) that corresponds to a perfect positioning of the steel frame in the mid-plane of the panel. These results show that, even though a millimeter positioning was achieved, it is not sufficient to consider one single value for α. However, to get a first order solution, the hypothesis $\delta = h/2$ could have been used to analyze the tests in a classical Weibull diagram (i.e., $\ln\left[\ln\left\{1/(1-P_F)\right\}\right]$ vs. $\ln\sigma_F$). This assumption was made in the *a priori* analysis of single and multiple cracking of lightly reinforced microconcrete panels.

Since each experiment has a different value of α, the only way to treat globally the scatter is to resort to the Weibull stress [Eqn. (5)] so that all data can be compared with one another. When the values of α and β change, the loading pattern is modified and one experiment cannot be compared with another one since the stress heterogeneity factor [Eqn. (28)] and the effective volume [Eqn. (3)] change. This is all the more important as a significant variation of α was obtained (Fig. 7). For each cracking event, the values of α and β are determined from the analysis of the strain measurements as explained in the previous sub-section. By knowing the Weibull modulus m (i.e., $m = 7.3$), the stress heterogeneity is determined [Eqn. (28)], as well as the effective volume [Eqn. (3)] and the corresponding Weibull stress [Eqn. (5)]. All the Weibull stresses are ranked in ascending order so that Eqn. (8) can be used to evaluate all the failure probabilities. Figure 10 summarizes all the experimental observations in the modified Weibull plot (i.e., $\ln\left[\ln\left\{1/(1-P_F)\right\}\right]$ vs. $\ln\sigma_w$). All experimental data are located above the curve given by the Weibull model identified with the

flexure experiments. It therefore constitutes a lower estimate. This can be shown when fitting the experimental data with the same Weibull modulus (i.e., $m = 7.3$) and leaving the scale parameter free. As a consequence, the Weibull stresses remain the same since the ratio V_{eff}/V_0 only depends on the Weibull modulus m. A value $\hat{S}_0 = 4.8\,\text{MPa}$ is found for the same reference volume (i.e., $V_0 = 20\,\text{cm}^3$) with a correlation coefficient equal to 0.96. It can be noted that the average effective volume observed in the experiments prior to first cracking, $V_{eff} \approx 240\,\text{cm}^3$, is at least two orders of magnitude larger than those that correspond to the unreinforced beams tested in flexure. Consequently, an extrapolation of the model to these very different scales may explain the 20% difference in scale parameter (i.e., $\hat{S}_0 = 4.8\,\text{MPa}$ instead of $S_0 = 4.0\,\text{MPa}$ for the unreinforced microconcrete). Last, the fact that the same Weibull modulus could be used in all the analyses indicates that the overall scatter remains similar even though the effective volumes are significantly different.

Finally, an *a posteriori* analysis of the cracking regimes is performed. It can be noted that this analysis is delicate since it needs a good evaluation of the stress field pattern because the effective volume and the corresponding failure stresses are dependent upon these quantities. Contrary to the previous analysis, the only knowledge of the Weibull stress is not sufficient to analyze the occurrence of the two regimes. A simplified path will be followed. By assuming a *representative* effective volume (e.g., the average effective volume observed in the experiments prior to first cracking, that is such that $V_{eff}/V_0 = 12$), Eqn. (18) can be rewritten as

$$f_{cr}(P_{cr}) = \left(\frac{\sigma_{su}}{\hat{S}_0 \left(\frac{V_0}{V_{eff}} \right)^{1/m} \left[-\ln(1 - P_{cr}) \right]^{1/m}} + 1 - \frac{E_s}{E_c} \right)^{-1} . \qquad (30)$$

Figure 11 shows the prediction of the critical volume fraction as a function of the first cracking probability. It allows one to conclude that for a volume fraction $f = 0.005$, about 75% of the samples are likely to experience multiple cracking. In practice a value of 85% was found. By remembering that the present analysis is only a first order evaluation, it can be concluded that the predictions are in reasonable agreement with the experimental observations, provided the corrected Weibull parameters are considered. If the Weibull parameters identified with the flexure data had been used, it would have been possible to state that multiple cracking was even likelier than observed.

CONCLUSIONS

The aim of the work reported herein was to analyze cracking in lightly reinforced microconcrete panels by using a Weibull model. To perform this type of analysis, 160 experiments were carried out on microconcrete alone. It was shown that a classical Weibull approach could be used to model single cracking of unreinforced beams. In particular, the effect of volume change and load pattern (i.e., stress heterogeneity) could be accounted for in a reasonable manner. More importantly, it was shown that all experimental data could be plotted in a unique *modified* Weibull diagram in which the relevant stress to consider is the so-called *Weibull stress*. This is the first important result of the paper. Furthermore, the aggregate distribution was controlled in this work. It followed that the typical aggregate size was of the order of 2.8 mm (i.e., 11 % of the smallest characteristic size of the samples) so that it is assumed that a macroscopic stress analysis was sufficient to capture the main fracture features on unreinforced microconcrete. Additional investigations may be undertaken to analyze large volumes of material to check the validity of the Weibull model. The ultimate strength of the reinforcements was considered as deterministic.

From these data, it was assumed for the 33 tested panels that the behavior of each constituent is linear elastic. Based on a probabilistic perspective, an *a priori* analysis predicted that a multiple cracking regime was expected and it was confirmed *a posteriori* by the experiments. The present analysis accounts for the scatter of failure stresses of the microconcrete matrix. Even though the matrix underwent multiple cracking, its behavior was assumed to be linear elastic and described, locally, by a weakest link approximation associated to a Weibull model with different *effective volumes*. Moreover, one had to resort to a modified Weibull diagram. In the present case, this was the *only* way to analyze all successive cracking events in a single diagram since each experiment was unique in terms of stress heterogeneity. Consequently, a *conventional* Weibull analysis could not be used. The use of the Weibull stress is therefore unavoidable in the present case. Otherwise the different test results cannot be compared with each other. This constitutes a further validation of the approach proposed herein.

The levels of cracking stresses could be predicted in a good way by assuming that the mechanical properties of the matrix were 20% higher than those of microconcrete alone. Consequently, the use of the data of microconcrete alone would have resulted in conservative estimates of the cracking levels of the reinforced panels. When the first cracking event is used as a design parameter, a lower bound can be expected. Additional investigations may be undertaken to analyze larger panels to confirm this trend.

Since the reinforcement was obtained by a grid of wires, it is believed that the role of the interface between longitudinal reinforcements and the surrounding matrix is minimal compared with the role played by the transverse reinforcements prescribing the longitudinal strains. As a consequence, the mechanical analysis was simple: each cracking event leads to the loss of a height at least equal to one reinforcement spacing, depending on the location of the crack. There was no need to identify the properties of the interface, other than checking

that the reinforcements were able to sustain the load carried by the matrix prior to cracking. In the present analysis, a discrete description of cracking was proposed since the maximum number of events was small (i.e., at most 3). There was therefore no need to use a continuum description based upon a damage parameter modeling matrix-cracking (Hild et al. 1996).

ACKNOWLEDGEMENTS

This work was supported by a CNPq (Brazil) / CNRS (France) cooperation grant between the Department of Structural Engineering (University of São Paulo at São Carlos) and LMT-Cachan (ENS de Cachan / CNRS-UMR 8535 / Université Paris 6). Discussions with the MMP group at LMT-Cachan are gratefully acknowledged.

APPENDIX. REFERENCES.

Abramowitz, M., and Stegun, I. A. (1965). *Handbook of Mathematical Functions*. Dover Publications, Inc., New York (USA).

Absi, J., Fournier, P., and Glandus, J. C. (1999). "Influence of experimental parameters on the estimated value of Weibull modulus." *J. Mat. Sci.*, 34, 1219-1227.

Aveston, J., Cooper, G. A., and Kelly, A. (1971). "Single and Multiple Fracture." *Proceedings National Physical Laboratory: Properties of Fiber Composites*, IPC Science and Technology Press, Surrey (UK), 15-26.

Aveston, J., and Kelly, A. (1973). "Theory of Multiple Fracture of Fibrous Composites." *J. Mater. Sci.*, 8, 352-362.

Balaguru, P. N., and Shah, S. P. (1992). *Fiber Reinforced Cement Composite*. McGraw Hill, New York (USA).

Bažant, Z. P. (1984). "Size Effect in Blunt Fracture: Concrete, Rock, Metal." *ASCE J. Eng. Mech.*, 110, 518-535.

Bažant, Z. P. (2000). "Size Effect." *Int. J. Solids Struct.*, 37, 69-80.

Bažant, Z. P., and Pijaudier-Cabot, G. (1989). "Measurement of Characteristic Length of Nonlocal Continuum." *ASCE J. Eng. Mat.*, 115 (4), 755-767.

Beremin, F. M. (1983). "A Local Criterion for Cleavage Fracture of a Nuclear Pressure Vessel Steel." *Metallurgical Transactions A*, 14A, 2277-2287.

Boudon–Cussac, D., Hild, F., and Pijaudier-Cabot, G. (1999). "Tensile Damage in Concrete: Analysis of an Experimental Technique." *J. Eng. Mech., ASCE*, 125 (8), 906-913.

Davies, D. G. S. (1973). "The Statistical Approach to Engineering Design in Ceramics." *Proc. Brit. Ceram. Soc.*, 22, 429-452.

El Debs, M. K. (2000). *Concreto pré-moldado : fundamentos e applicações*. Projeto Reenge, São Carlos, EESC-USP (Brasil).

Freudenthal, A. M. (1968). "*Statistical Approach to Brittle Fracture*." In: Fracture, Academic Press, New York (USA), 591-619.

Gere, J. M., and Timoshenko, S. P. (1997). *Mechanics of Materials*. PWS Publishers, 4th edition, Boston (USA).

Hanai, J. B., and El Debs, M. K. (1994). "The Future of Ferrocement in Civil Engineering." *Proceedings Ferrocement (Proceedings of the Vth Int. Symposium on Ferrocement, Manchester (UK), 6-9 sept. 1994)*, E&FN SPON, London (UK), 17-26.

Hild, F., Billardon, R., and Marquis, D. (1992). "Hétérogénéité des contraintes et rupture des matériaux fragiles." *C. R. Acad. Sci. Paris*, t. 315 (Série II), 1293-1298.

Hild, F., Burr, A., and Leckie, F. A. (1996). "Matrix Cracking and Debonding in Ceramic-Matrix Composites." *Int. J. Solids Struct.*, 33 (8), 1209-1220.

Jayatilaka, A. de S. (1979). *Fracture of Engineering Brittle Materials*. Applied Sciences Publishers, London (UK).

Kadlecek, V., and Spetla, Z. (1967). "Effect of Size and Shape of Test Specimens on the Direct Tensile Strength of Concrete." *Bull. RILEM*, 36, 175-184.

Kurkjian, C. R. (1985). *Strength of Inorganic Glass*. Plenum Press, New York (USA).

Lambot, J. L. (1855). "*Ferciment*." French patent.

L'Hermite, S. (1960). "Volume Changes in Concrete." *Proceedings 4th International Symposium on the Chemistry of Cement*, 659-702.

L'Hermite, S. (1973). "Influence de la dimension absolue sur la résistance de flexion." *Annales de l'I.T.B.T.P.*, 309-310, 39-41.

Marrey, B. (1995). *Les ponts modernes - vingtième siècle*. Picard éditeurs, Paris (France).

Mazars, J., and Berthaud, Y. (1989). "Une technique expérimentale appliquée au béton pour créer un endommagement diffus et mettre en évidence son caractère unilatéral." *C. R. Acad. Sci. Paris*, Série II (t. 308), 579-584.

Mazars, J., Berthaud, Y., and Ramtani, S. (1990). "The Unilateral Behavior of Damaged Concrete." *Eng. Fract. Mech.*, 35 (4/5), 629-635.

Naaman, A. E. (2000). *Ferrocement and Laminated Cementious Composites*. Techno Press 3000, Ann Arbor (USA).

Nervi, P. L. (1951). "Il ferro-cemento : sue caratteristiche e possibilità." *L'ingegniere*, 25 (1), 17-25.

Silva, A. R. C. (2002). "*Uma abordagem probabilista de ruptura de painéis tracionados de concreto de granulometria fina armados com telas soldadas*." PhD thesis, University of São Paulo (in Portuguese).

Weibull, W. (1939). "*A Statistical Theory of the Strength of Materials*." Report 151, Roy. Swed. Inst. Eng. Res.

APPENDIX. CALCULATION OF STRESS HETEROGENEITY FACTORS

Let us consider a beam loaded in four-point flexure (Fig. 12). By using a beam theory solution (Gere and Timoshenko 1997), the stress field is unidimensional in the *y*-direction $\sigma_{yy}(x,y)$, linear with the *x* and *y* coordinates and independent of the *z* coordinate

$$\sigma_{yy}(x,y)=\begin{cases} -\sigma_F \dfrac{2xy}{ah} & \text{if } 0 \le y \le a, \\ -\sigma_F \dfrac{2x}{h} & \text{if } a \le y \le a+c, \\ -\sigma_F \dfrac{2x[(2a+c)-y]}{ah} & \text{otherwise.} \end{cases} \tag{31}$$

Since the stress field is unidirectional and normal, the equivalent stress σ_e is equal to σ_{yy}. One only considers the positive part of the equivalent stress [Eqn. (3)], the integration along the *x* direction is only carried out when *x* is negative. The stress heterogeneity factor [Eqn. (3)] can be calculated as

$$\begin{aligned} (2a+c)hwH_m = & \int_{-h/2}^{0}\int_{0}^{a}\int_{-w/2}^{w/2}\left(\frac{-2xy}{ah}\right)^m dxdydz \\ & + \int_{-h/2}^{0}\int_{a}^{a+c}\int_{-w/2}^{w/2}\left(\frac{-2x}{h}\right)^m dxdydz \\ & + \int_{-h/2}^{0}\int_{a+c}^{2a+c}\int_{-w/2}^{w/2}\left(\frac{-2x[(2a+c)-y]}{ah}\right)^m dxdydz \end{aligned}, \tag{32}$$

so that for any span ratio a/c

$$H_m = \frac{2a}{2a+c}\frac{1}{2(m+1)^2} + \frac{c}{2a+c}\frac{1}{2(m+1)}. \tag{33}$$

The case $a/c \to 0$ corresponds to pure flexure

$$H_m = \frac{1}{2(m+1)}. \tag{34}$$

When $a/c = 1$, Eqn. (10) is found. Finally when $c/a \to 0$, it corresponds to three-point flexure and Eqn. (11) is obtained.

When the strain field $\varepsilon_{yy}(x)$ is given by Eqn. (19), the corresponding uniaxial stress field $\sigma_{yy}(x)$ becomes

$$\sigma_{yy}(x) = \left[\frac{1+\alpha}{2} + (1-\alpha)\frac{x}{h}\right]\sigma_F \tag{35}$$

When $\alpha \geq 0$, the integration over x is carried out for any value of x

$$LhwH_m = \int_{-h/2}^{h/2}\int_{0}^{L}\int_{-w/2}^{w/2}\left[\frac{1+\alpha}{2} + (1-\alpha)\frac{x}{h}\right]^m dxdydz, \tag{36}$$

whereas, when $\alpha \leq 0$, the integration over x is carried out for any value of x greater than or equal to $-h(1+\alpha)/2(1-\alpha)$ so that the equivalent stress is positive

$$LhwH_m = \int_{-h(1+\alpha)/2(1-\alpha)}^{h/2}\int_{0}^{L}\int_{-w/2}^{w/2}\left[\frac{1+\alpha}{2} + (1-\alpha)\frac{x}{h}\right]^m dxdydz, \tag{37}$$

and Eqn. (23) is obtained.

APPENDIX. NOMENCLATURE

a = inner span;

b = distance from one side of the specimen;

$2c+a$ = outer span;

d = wire diameter;

E = Young's modulus of composite;

E_c, E_s = elastic moduli of concrete and steel, respectively;

E_h = equivalent Young's modulus;

f = volume fraction of reinforcements;

f_{cr} = critical volume fraction of reinforcements;

f_h = apparent surface fraction of reinforcements;

F = applied load;

h = thickness of the sample;

H_m = stress heterogeneity factor (Hild et al. 1992);

i = index;

L = length of the panel;

m = Weibull modulus;

N = number of samples;

P_F = cumulative failure probability;

P_{cr} = cracking probability;

S = spacing between wires;

S_0 = scale parameter (relative to a reference volume V_0);

$\hat{S}_0$ = corrected scale parameter (relative to a reference volume V_0);

V = loaded volume;

V_0 = reference volume;

V_c = volume of concrete;

V_{eff} = effective volume;

U_L = displacement measured on the left side of the specimen;

U_R = displacement measured on the right side of the specimen;

w = width of the sample;

x = normal direction (see Fig. 4);

y = loading direction and first wire direction (see Fig. 4);

z = second wire direction;

α = coefficient of flexure (i.e., if $\alpha = 1$, then no flexure is observed and if $\alpha = -1$, then pure flexure is obtained);

α_a = apparent coefficient of flexure;

β = flexure parameter in the longitudinal plane;

Γ = Euler function of the second kind (Abramowitz and Stegun 1965);

δ = eccentricity parameter (see Fig. 4);

ε_{yy} = normal strain in the loading direction (y);

$\varepsilon_{\max}$ = maximum normal strain in the loading direction (y);

$\bar{\varepsilon}_m$ = average strain in the matrix;

σ_c, σ_s = stress in concrete and in steel, respectively;

σ_{cu}, σ_{su} = failure stress of concrete and steel, respectively;

$\bar{\sigma}_{cu}$ = average failure stress of concrete;

$\sigma_e(\mathbf{x})$ = equivalent failure stress at location $\mathbf{x}$ (e.g., the local maximum principal stress);

σ_F = failure stress;

$\overline{\sigma}_F$ = average failure stress;

σ_{Fi} = ordered failure stress;

σ_w = Weibull stress;

σ_1 = maximum tensile stress in the matrix;

Σ = applied stress;

Σ_1 = average tensile stress;

Σ_{cr} = stress level at which matrix-cracking occurs;

Ω = domain;

θ = angle with respect to the axis of symmetry of the panel;

$\langle . \rangle$ = Macauley brackets.

FIGURE CAPTIONS

Figure 1: Cumulative failure probability vs. failure stress of four test series performed at different ages in 3-point flexure (loaded volume: 150 x 25 x 25 mm^3). No conclusive correlation can be found between age and failure stress level.

Figure 2: Experimental data for the four sets of experiments. For each set, the line corresponds to the best Weibull fit.

Figure 3: Modified Weibull plot (i.e., cumulative failure probability P_F versus Weibull stress σ_w) of all the test results obtained for two different sample sizes and two different loading types. The solid line corresponds to the Weibull model ($S_0 = 4\,\text{MPa},\ m = 7.3$).

Figure 4: Panel geometry (400 x 400 x 25 mm^3, $S = 100$ mm), section along one longitudinal wire axis and 300 mm long beam model, which is homogeneous in the *z*-direction, used to account for the eccentricity δ.

Figure 5: Elementary cell used in the analysis of single and multiple cracking regimes.

Figure 6: Single and multiple matrix-cracking regimes of a reinforced brittle matrix ($E_f = 215\,\text{GPa},\ E_m = 19\,\text{GPa},\ \sigma_{fu} = 870\,\text{MPa},\ S_0 = 4\,\text{MPa},\ m = 7.3$) for three different values (namely, 1, 10, 100) of dimensionless effective volumes V_{eff}/V_0.

When $f > f_{cr}$, a multiple cracking regime can be expected. Conversely, when $f \leq f_{cr}$, single cracking occurs.

Figure 7: Flexure parameter α vs. eccentricity δ. The crosses are experimental data. The experimental average $\overline{\alpha} = 0.33$ corresponds to an eccentricity $\delta = 2$ mm.

Figure 8: Location of the six displacement transducers used in the tests on the panels.

Figure 9: -a- Raw displacement measurements of the six transducers.

-b- Average of the three measurements on each surface of the panels. An apparent flexure parameter $\alpha_a \approx -0.24$ is obtained. The circles correspond to the first, second and third cracking events.

-c- Corrected strain on the surfaces of the panel. The actual flexure parameters being derived as $\alpha \approx 0.44$ and $\beta \approx 0.75$ for the first cracking stress.

Figure 10: Modified Weibull plot (i.e., cumulative failure probability P_F versus Weibull stress σ_w) corresponding to the first, second and third cracking stresses. The solid line corresponds to the Weibull parameters determined from the flexure data. The dashed line corresponds to the Weibull scale parameter determined by using the present data.

Figure 11: Single and multiple matrix-cracking regimes of the lightly reinforced panels ($E_f = 210\,\text{GPa}$, $E_m = 19\,\text{GPa}$, $\sigma_{fu} = 870\,\text{MPa}$, $\hat{S}_0 = 4.8\,\text{MPa}$, $m = 7.3$) when

$V_{eff}/V_0 = 12$. When $f > f_{cr}$, a multiple cracking regime can be expected. Conversely, when $f \leq f_{cr}$, single cracking occurs.

Figure 12: Beam geometry used to calculate stress heterogeneity factors in four-point flexure for different span ratios a/c.

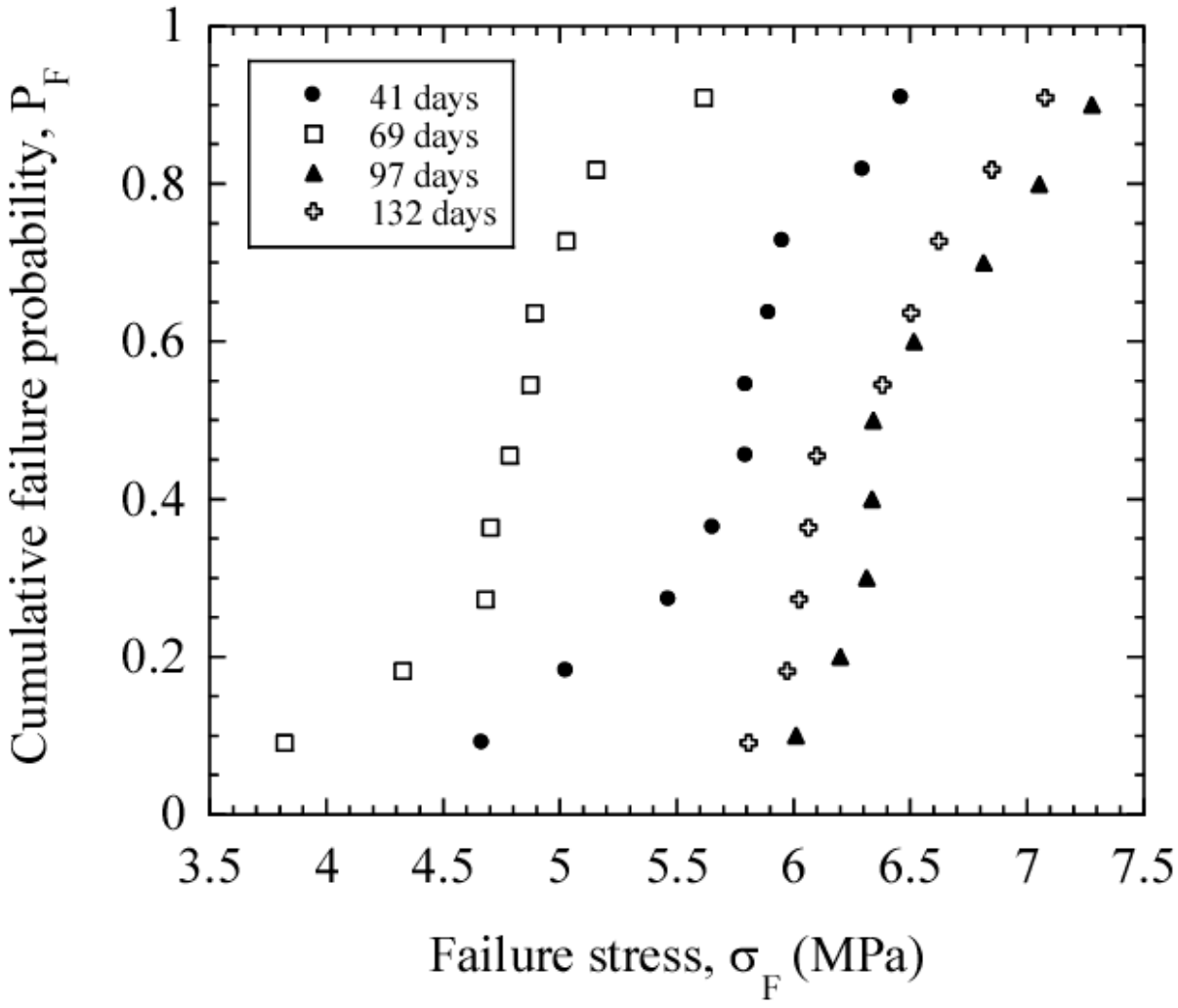

Figure 1: Silva et al.

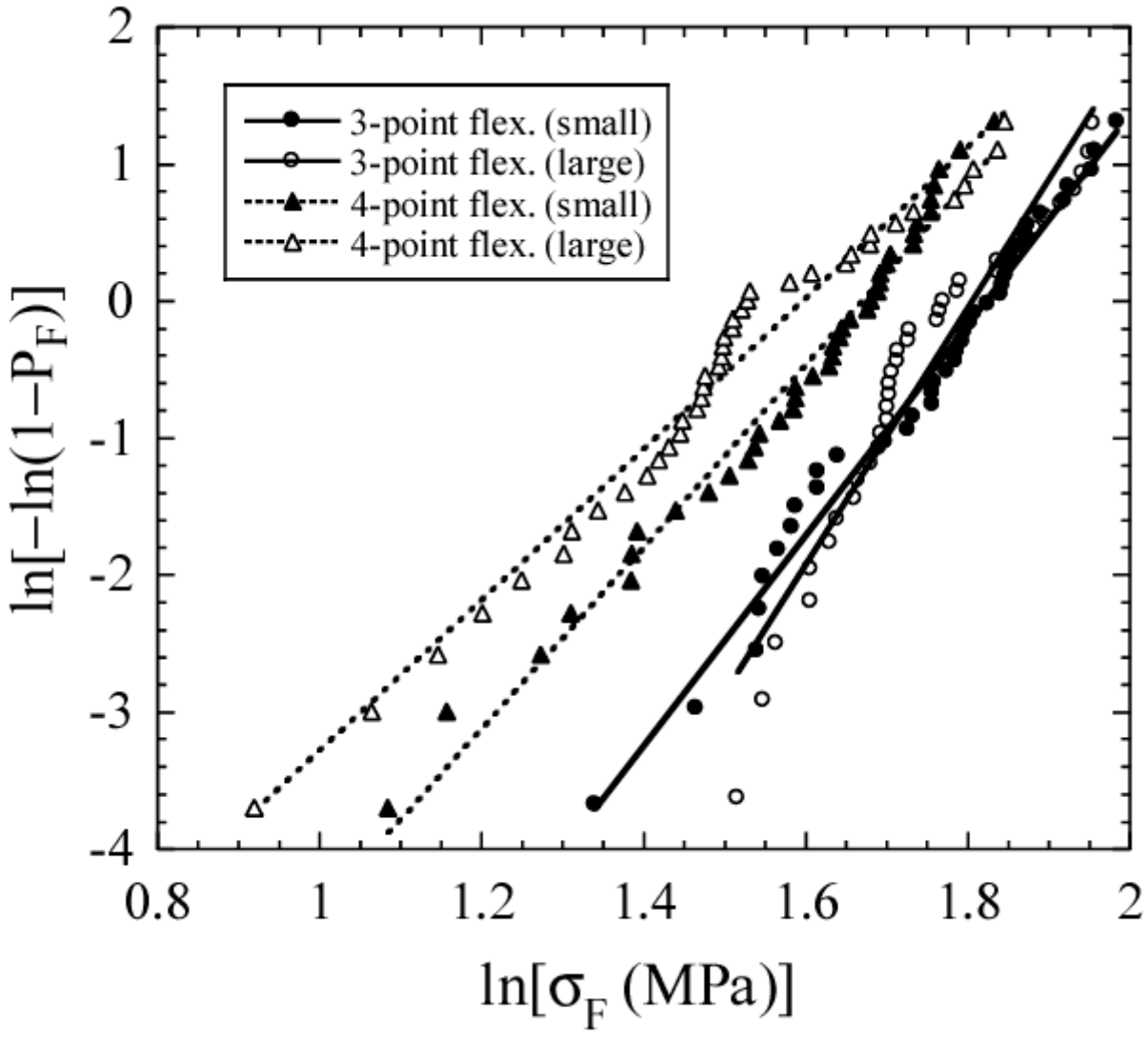

Figure 2: Silva et al.

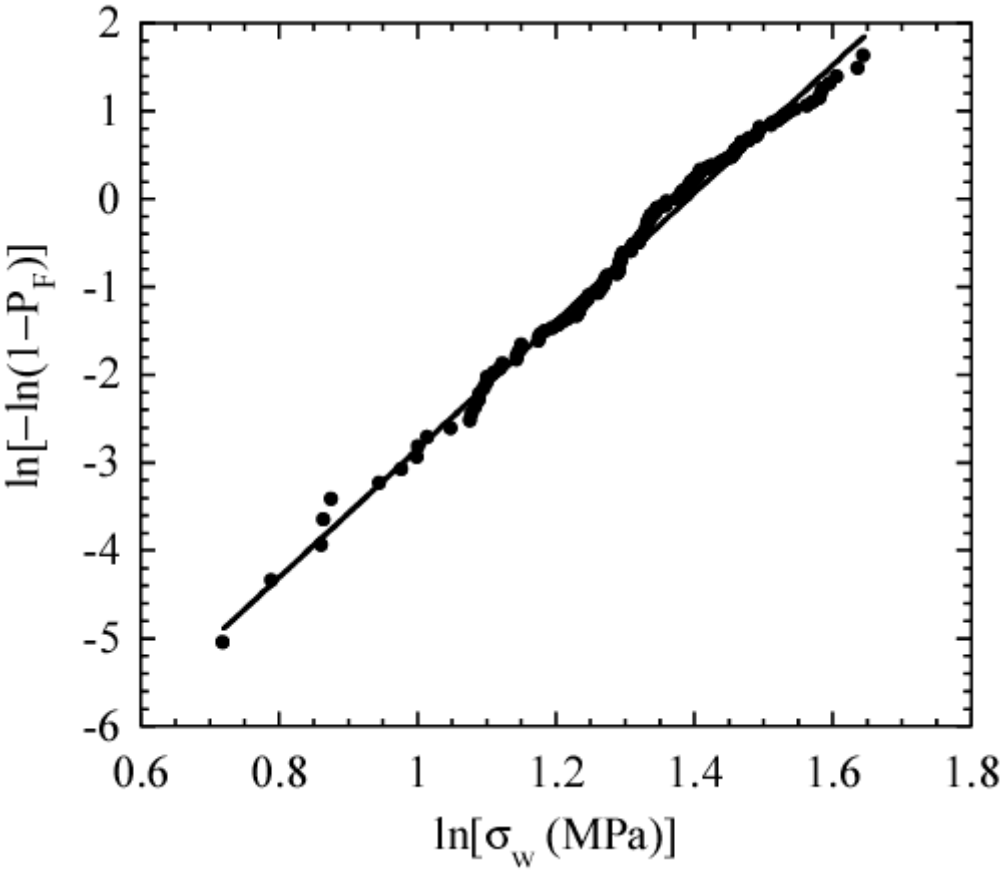

Figure 3: Silva et al.

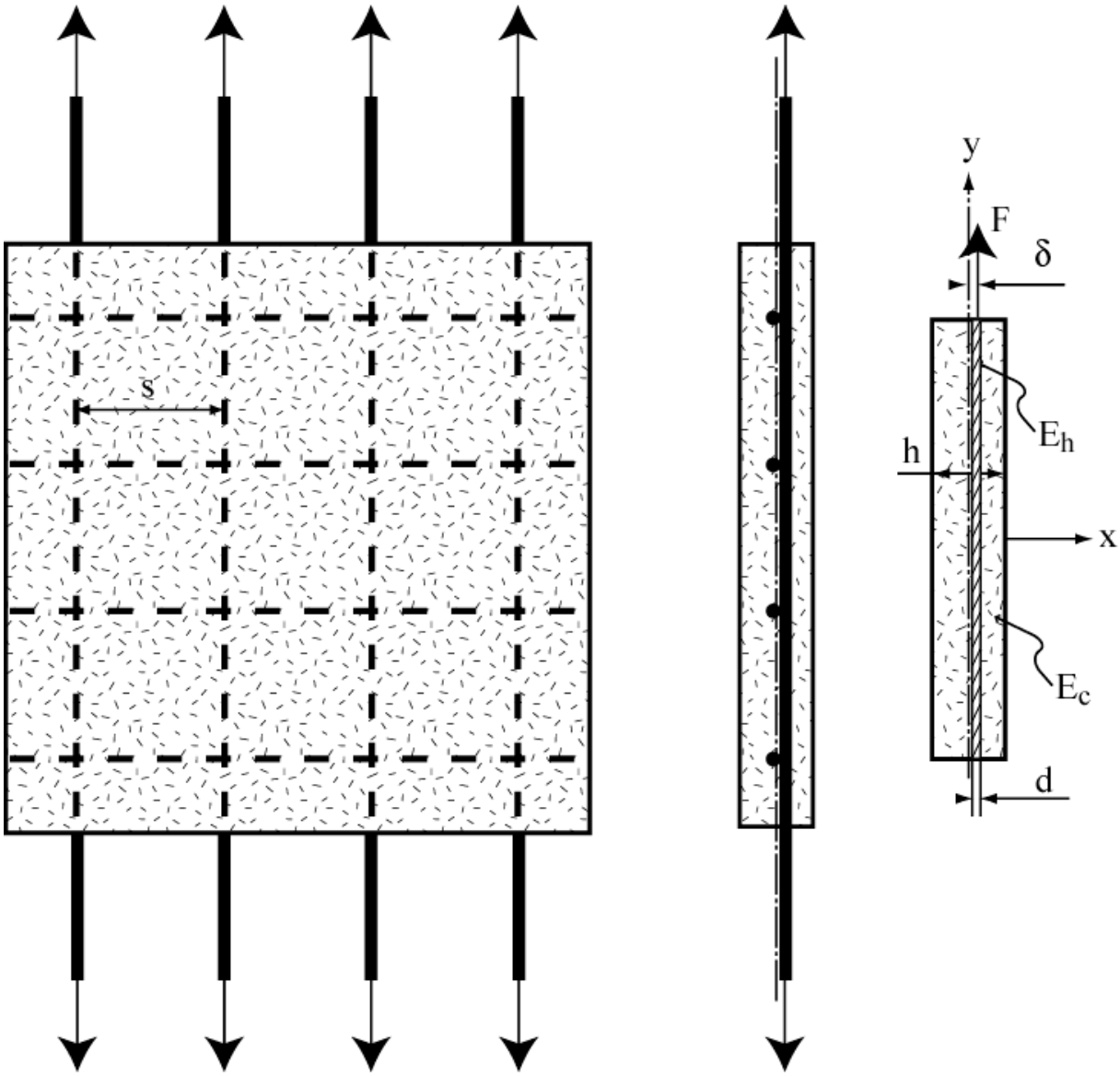

Figure 4: Silva et al.

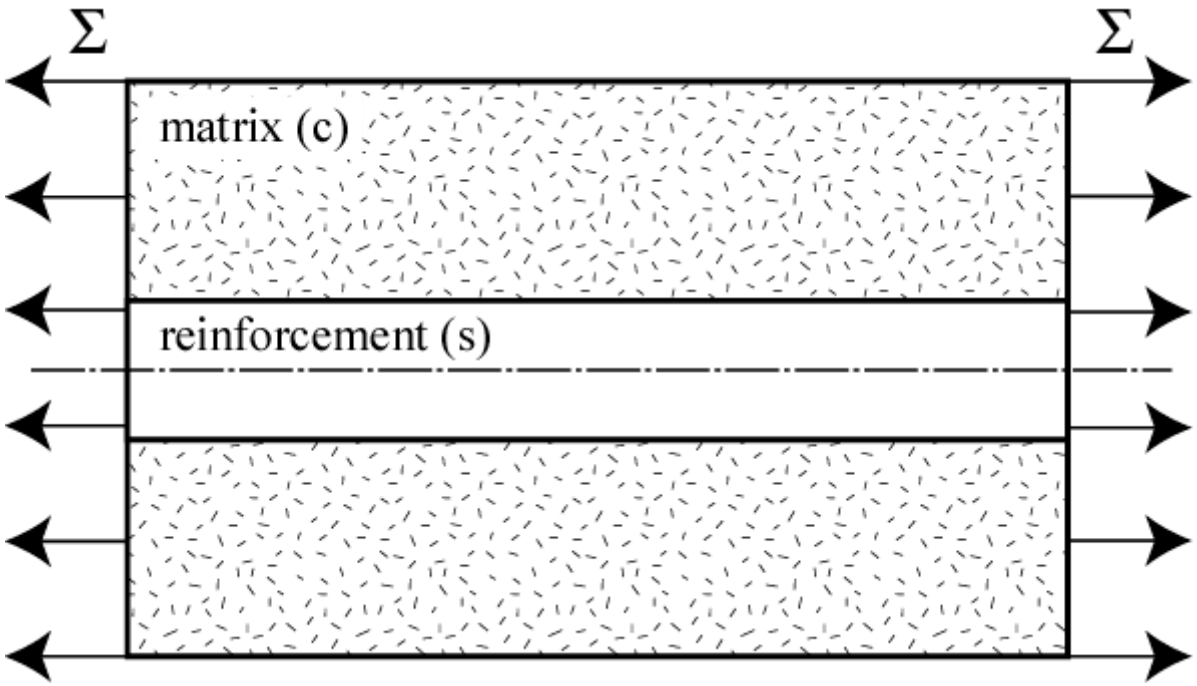

Figure 5: Silva et al.

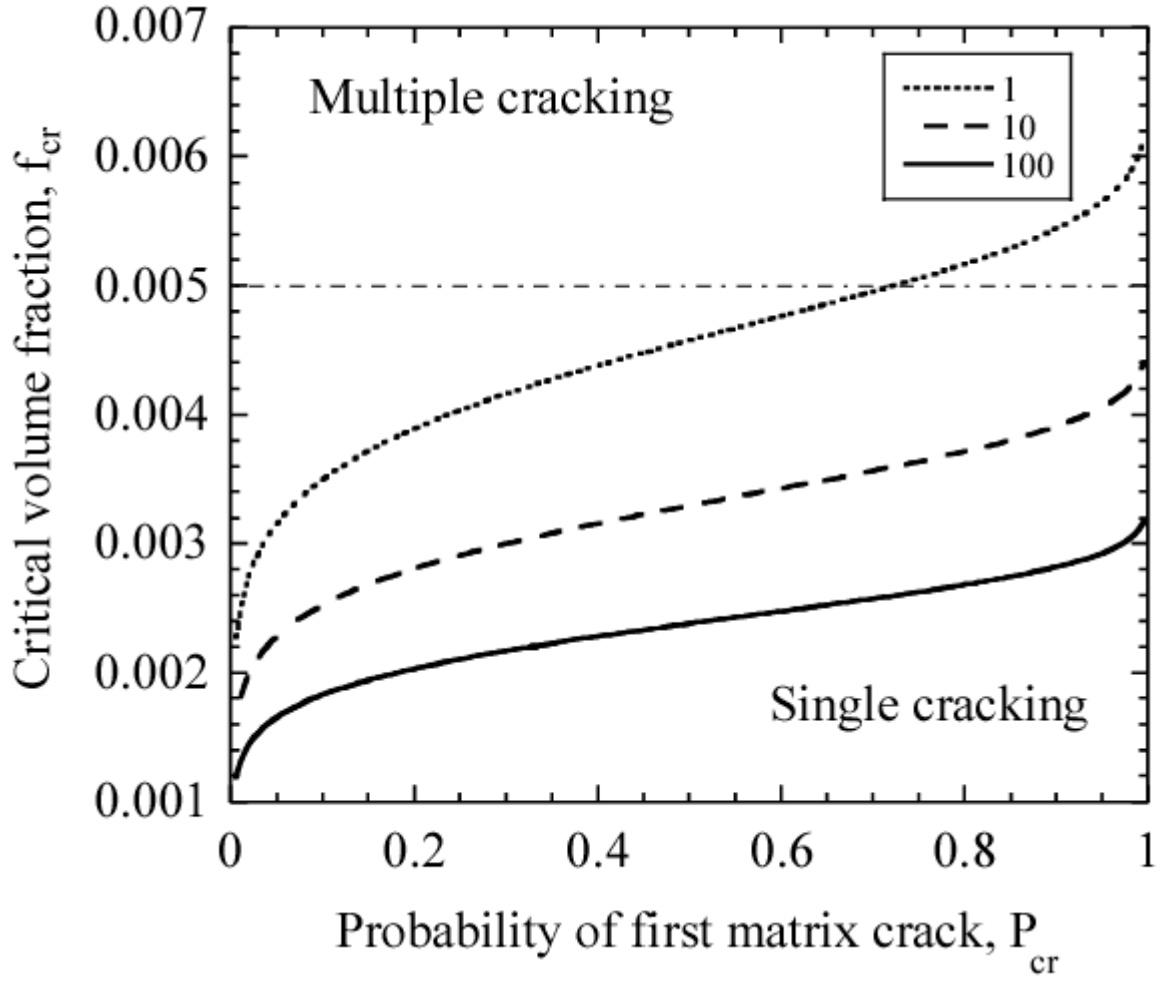

Figure 6: Silva et al.

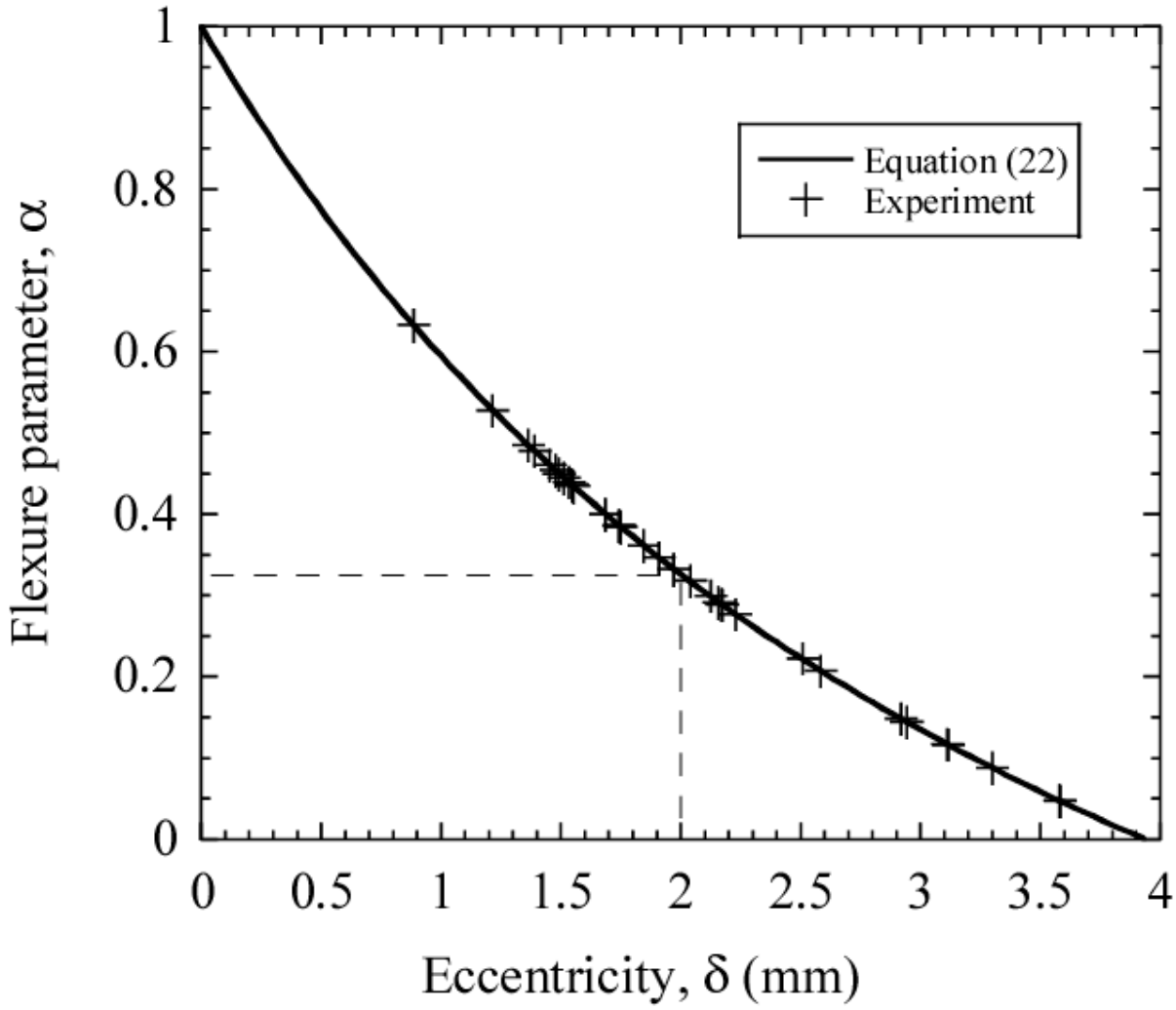

Figure 7: Silva et al.

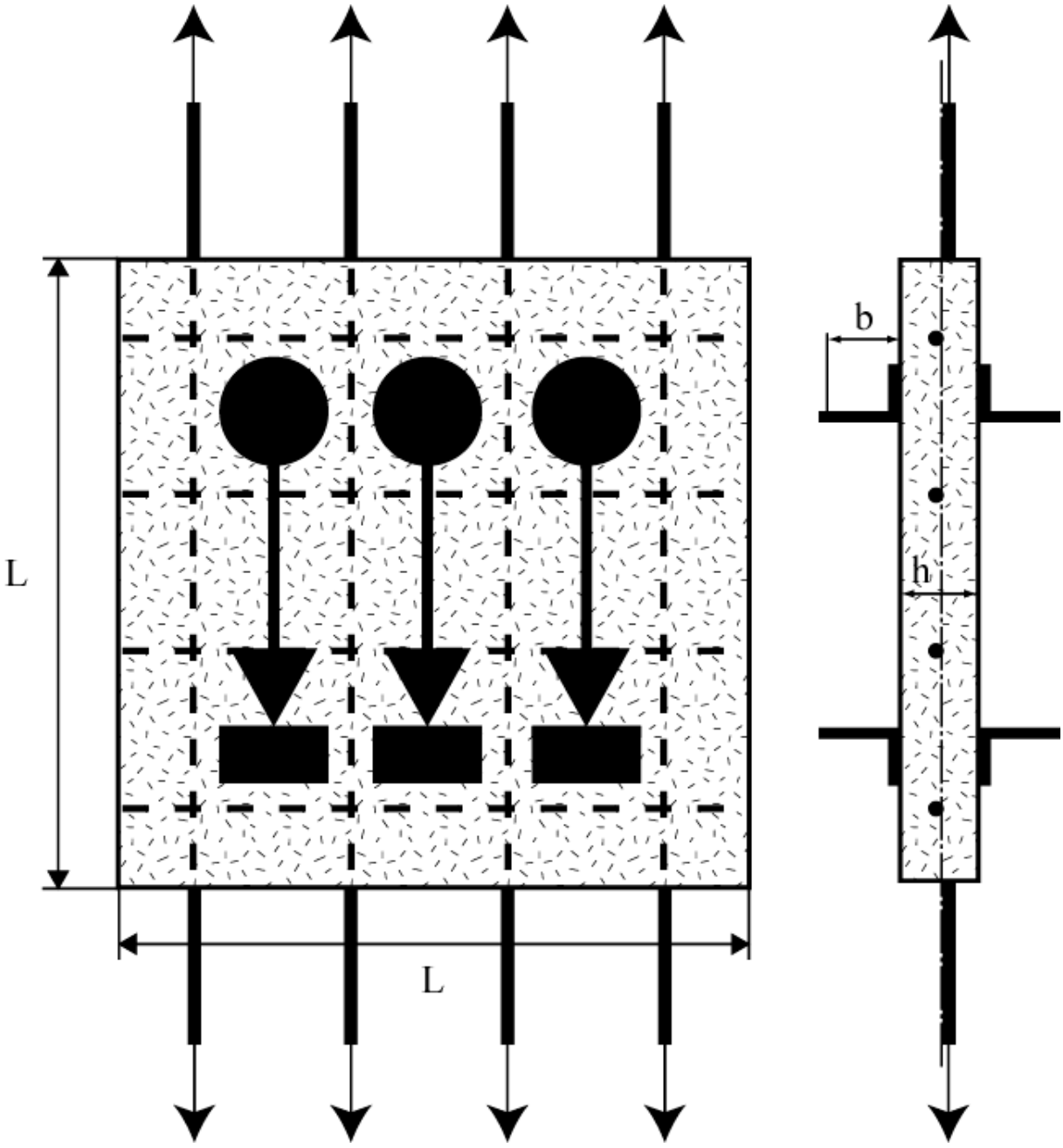

Figure 8: Silva et al.

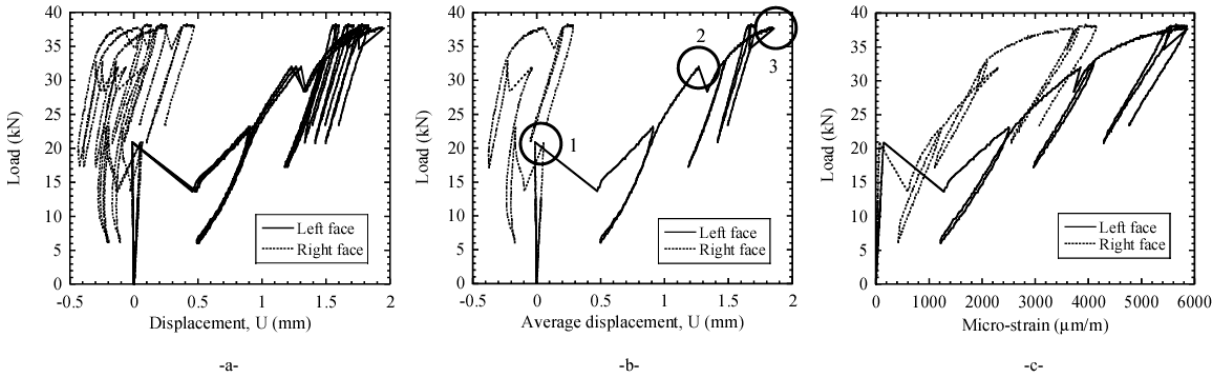

Figure 9: Silva et al.

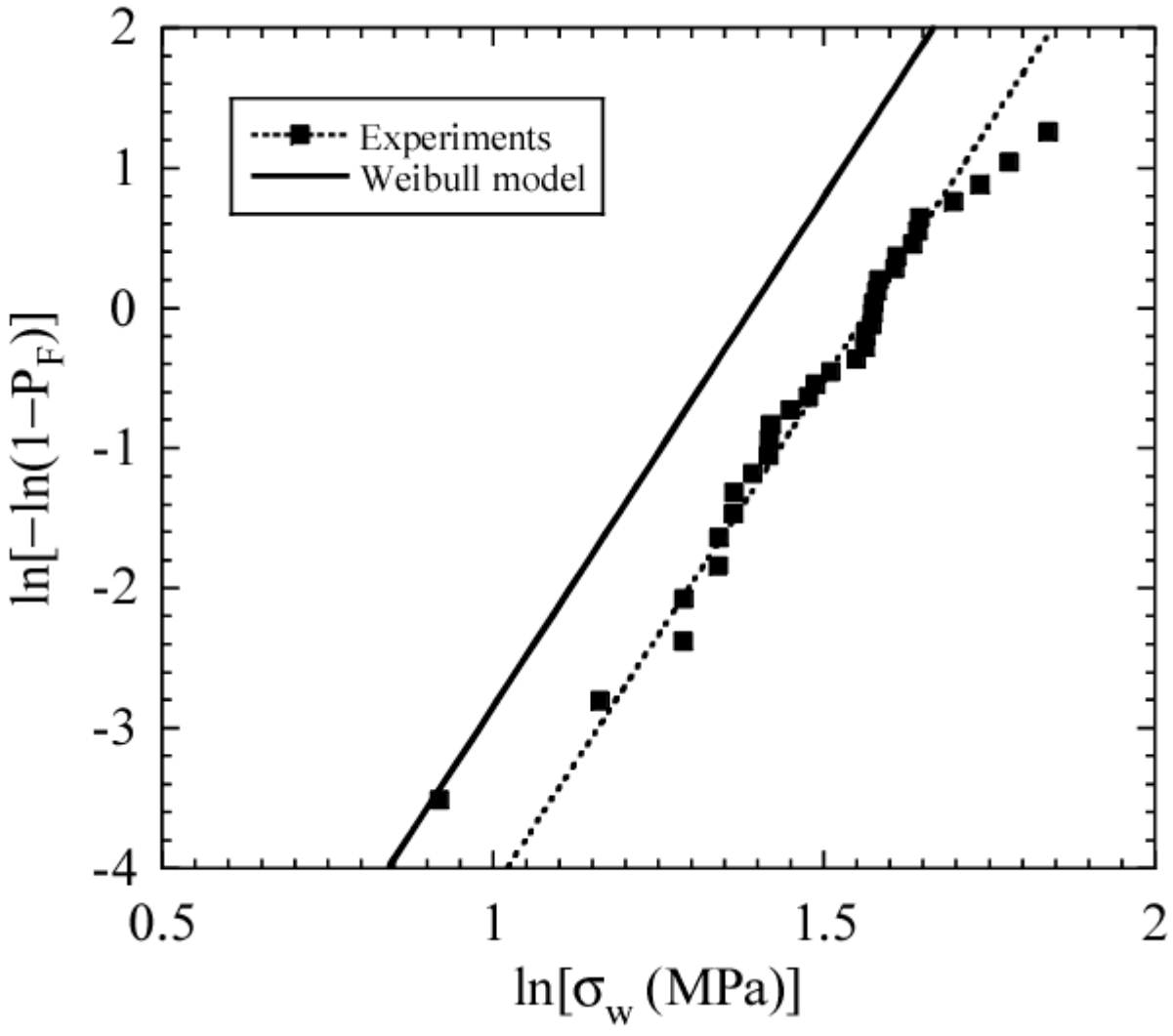

Figure 10: Silva et al.

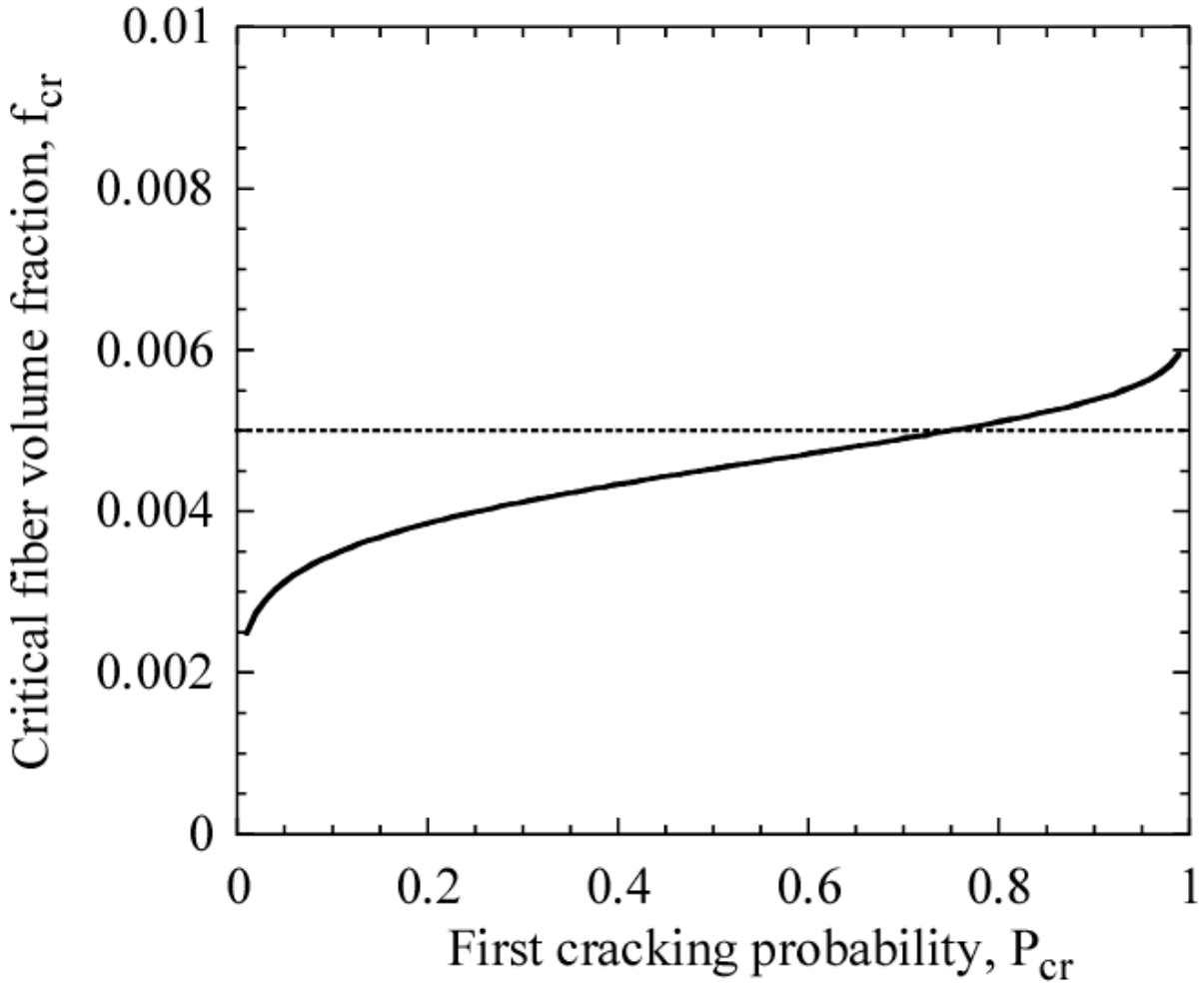

Figure 11: Silva et al.

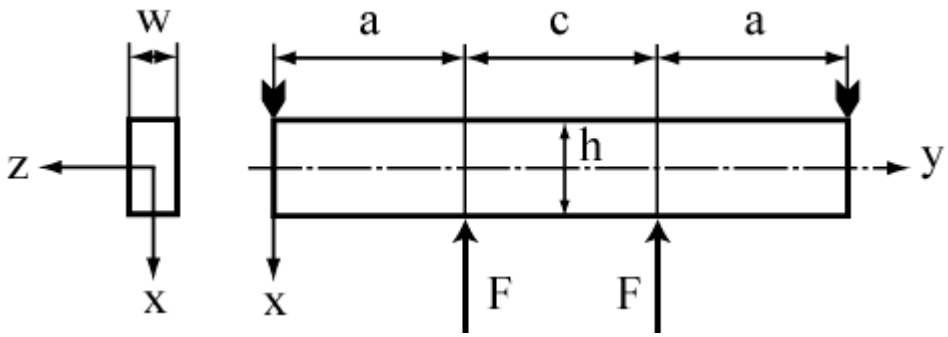

Figure 12: Silva et al.

TABLE CAPTION

Table 1: Distribution of sand size for the constituents used to make microconcrete.

Table 2: Distribution of aggregate size for the constituents used to make microconcrete.

Table 3: Weibull parameters of the four sets of flexural experiments on micro-concrete samples ($V_0 = 20\,\mathrm{cm}^3$). For the average failure stress, the value in parentheses corresponds to the prediction by the Weibull model ($m = 7.3$, $S_0 = 4\,\mathrm{MPa}$ and $V_0 = 20\,\mathrm{cm}^3$)

Table 4: Failure stress (average ± standard deviation) for the two different test series on steel wires.

Table 1: Silva et al.

Sieve size (mm)	Kept mass (g)	Mass distribution	Cumulative mass
1.2	23.4	2.3 %	2.3 %
0.6	277.3	27.8 %	30.1 %
0.3	484.6	48.5 %	78.6 %
0.15	202.0	20.2 %	98.8 %
Balance	11.9	1.2 %	100 %

Table 2: Silva et al.

Sieve size (mm)	Kept mass (g)	Mass distribution	Cumulative mass
4.8	1.2	0.1 %	0.1 %
2.4	640.9	64.1 %	64.2 %
1.2	289.4	29.0 %	93.2 %
0.6	44.0	4.4 %	97.6 %
0.3	14.0	1.4 %	99 %
0.15	6.2	0.6 %	99.6 %
Balance	3.7	0.4 %	100 %

Table 3: Silva et al.

Sample size (mm^3)	Type of test	Mean failure stress $\overline{\sigma}_F$ (MPa)	Weibull modulus m	Scale parameter S_0 (MPa)
25 x 25 x 170	4-point flexure	5.0 (5.1)	6.6	3.9
	3-point flexure	5.8 (6.0)	7.7	3.9
25 x 25 x 320	4-point flexure	4.6 (4.6)	5.5	4.0
	3-point flexure	5.8 (5.4)	9.4	4.4

Table 4: Silva et al.

Sample length (mm)	Failure stress (MPa)	Young's modulus (GPa)
100	878 ± 11	212 ± 13
200	866 ± 31	222 ± 32